BIOLOGY OF REPRODUCTION (2012) **87**(6):132, 1–10
Published online before print 10 October 2012.
DOI 10.1095/biolreprod.112.103366

Microbial Products Alter the Expression of Membrane-Associated Mucin and Antimicrobial Peptides in a Three-Dimensional Human Endocervical Epithelial Cell Model[1]

Andrea L. Radtke,[3] Alison J. Quayle,[4] and Melissa M. Herbst-Kralovetz[2,3]

[3]*Department of Basic Medical Sciences, University of Arizona College of Medicine–Phoenix, Phoenix, Arizona*
[4]*Department of Microbiology, Immunology, and Parasitology, Louisiana State University Health Sciences Center, New Orleans, Louisiana*

ABSTRACT

Our understanding of the mechanisms that regulate tissue-specific mucosal defense can be limited by the lack of appropriate human in vitro models. The endocervix lies between the microbe-rich vaginal cavity and the relatively sterile endometrium and is a major portal of entry for *Chlamydia trachomatis*, *Neisseria gonorrhoeae*, *Mycoplasma genitalium*, human immunodeficiency virus (HIV), and herpes simplex virus (HSV) infection in women. The endocervix is lined with a simple epithelium, and these cells produce mucus, which plays a key role in immune defense and reproduction. Here we describe the development of a human three-dimensional endocervical epithelial cell model generated by rotating wall vessel bioreactor technology. The model is composed of cellular aggregates that recapitulate major structural and barrier properties essential for the function and protection of the endocervix, including junctional complexes, microvilli, innate immune receptors, antimicrobial peptides, and mucins, the major structural component of mucus. Using this model, we also report, for the first time, that the membrane-associated mucin genes *MUC1*, *MUC4*, and *MUC16* are differentially regulated in these aggregates by different bacterial and viral products. Differential induction of antimicrobial peptides was also observed with these products. Together these data define unique and flexible innate endocervical immune signatures that follow exposure to microbial products and that likely play a critical role in the outcome of pathogen challenge at this site.

3-D organotypic epithelial cell (EC) model, endocervix, female reproductive tract, innate immunity, mucosal surfaces, rotating wall vessel (RWV) bioreactor, toll-like receptors (TLR)

INTRODUCTION

The female reproductive tract (FRT) is a complex and dynamic biosystem of cells that must be responsive to changing environmental conditions such as hormone fluxes, commensal flora, and challenge by sexually transmitted pathogens [1, 2]. The FRT can be divided into regions based on the structure and functions of the cells that populate each site. The lower FRT, which includes the vagina and ectocervix, is covered with multiple layers of stratified squamous epithelial cells (EC) [2, 3]. This region is a major portal to the external environment and is repeatedly exposed to potentially damaging factors such as pathogens, chemicals, and physical stresses [1, 4–6]. In contrast, the upper FRT, which includes the uterus, endometrium, fallopian tubes, and endocervix, is composed of a single layer of columnar EC that mostly maintains a relatively sterile environment, with intermittent invasions of ascending microorganisms (both commensal and pathogenic) from the lower FRT [1, 3, 7–10].

The endocervix has a unique role in the FRT in that it serves as an interface between the relatively sterile upper and nonsterile lower portions of the tract; this separation is critical in maintaining the general function of the tissues [3, 7, 9, 11]. Endocervical EC attributes that limit microbial access and establishment of infection include tight intercellular junctions, production of mucus, and innate immune mediators [1, 8]. With respect to the first attribute, EC intercellular junctions maintain the integrity and organization of epithelia by regulating molecule translocation and by providing a physical barrier against microbe invasion [4, 8]. The relative impermeability of this endocervical epithelial barrier contrasts with the multilayered lower tract epithelium that commonly allows molecules and microbes to breach its uppermost apical layers [4, 5].

Mucus is also critical in establishing a protective barrier against molecules and microbes that are present at mucosal sites, and endocervical EC represent the primary source of mucus in the FRT [2, 12–14]. Mucins are large O-linked glycosylated proteins that are the major structural protein of mucus, and to date, 19 mucins have been identified through cDNA cloning [12, 15, 16]. Mucins can be categorized as gel-forming (secreted), membrane-associated, or small soluble mucins, and mucin profiles are site-specific [12, 13, 17–19]. Mucus not only forms a physical protective barrier against external environmental challenges but also houses an array of antimicrobial molecules [1, 18].

Antimicrobial peptides (AMPs) are potent broad spectrum antimicrobial proteins that disrupt microbial membranes and metabolic processes and can be found concentrated in the mucus bathing mucosal surfaces [1, 20]. Much of the knowledge about mucin and AMP expression and regulation has been gained by studies of the gastrointestinal (GI) tract [18]. Recent studies, however, provide evidence for site-specific differences in expression between the molecules in the upper FRT and for the fact that these differ from the GI tract and other mucosal surfaces [1, 7, 9, 21]. While elegant studies investigating AMP function and hormonal regulation of mucins in the FRT have been undertaken, there remains a gap in our

[1]Supported by an Alternatives Research Development Foundation grant to M.M.H.-K. and National Institutes of Health grant AI095859 to A.J.Q.
[2]Correspondence: Melissa M. Herbst-Kralovetz, Department of Basic Medical Sciences, University of Arizona College of Medicine–Phoenix, 445 N. 5th St., TGen Bldg., 3rd Floor, Phoenix, AZ 85004-3902.
E-mail: mherbst1@email.arizona.edu

Received: 12 July 2012.
First decision: 2 August 2012.
Accepted: 5 October 2012.

eISSN: 1529-7268 http://www.biolreprod.org
ISSN: 0006-3363

knowledge of how microbes regulate mucins and key innate mediators at this site [1, 8, 21, 22].

Previously, we developed and characterized a three-dimensional (3-D) vaginal EC model that forms a stratified squamous epithelium and exhibits ultrastructural features (microvilli, tight junctions, secretory vesicles, and microridges), mucus production, and barrier function that recapitulates the in vivo tissue [23]. Using this rotating wall-vessel (RWV) bioreactor technology, we constructed a human 3-D organotypic endocervical EC model that exhibits critical hallmarks of endocervical EC differentiation including apical-basal cellular polarity, formation of microvilli, secretory vesicles, desmosomes, and secretory material [2, 3, 17]. Systematic profiling of mucins and AMPs by quantitative RT-PCR also revealed similar levels of expression, as previously reported in endocervical tissue and secretions [12, 19]. We also investigated the mechanisms by which the endocervix regulates these key innate immune defenses following microbe challenge. This led us to identify unique endocervical innate immune signatures following exposure to specific viral and bacterial products. In summary, the 3-D human endocervical EC model provides the field with a physiologically relevant and complementary tool for the study of innate immune barrier and cellular responses of the endocervix and has identified key endocervical epithelial innate mediators that respond to microbial challenge.

MATERIALS AND METHODS

Human Endocervical EC Culture

The characterized endocervical EC line (A2EN) generated from human endocervical explant tissue, as previously described [22, 24], was grown in keratinocyte serum-free medium (Invitrogen, Carlsbad, CA) supplemented with 5 ng ml^{-1} human recombinant epidermal growth factor (Gibco, Grand Island, NY), 50 μg ml^{-1} bovine pituitary extract (Gibco), 22 mg ml^{-1} $CaCl_2$ (Sigma-Aldrich, St. Louis, MO), and 100 μg ml^{-1} Primocin (InvivoGen, San Diego, CA) [22, 24]. All cell quantification assays were performed using trypan blue exclusion staining and were quantified with the Countess (Invitrogen) automated cell counter following dissociation using 0.25% trypsin (Mediatech, Manassas, VA).

Generation of the 3-D Human Endocervical Model

Construction of the 3-D endocervical EC model was performed as previously described and demonstrated [23, 25, 26]. Briefly, A2EN cells were initially grown as monolayers (ML) in tissue culture flasks as described above and trypsinized, and single-cells suspensions (1×10^7 cells) were combined with 0.3 g of type 1 collagen-coated dextran microcarrier beads (Cytodex-3; Sigma-Aldrich). The cell-bead suspension was seeded into an RWV bioreactor vessel (Synthecon, Houston, TX); and the vessel was filled with cell culture medium, placed on a rotator base, and set to rotate at 20 rpm. After 4–5 days of culture and then every day afterward until harvest, 80% of medium was removed and replaced with fresh medium. After 29–35 days of culturing endocervical cells in the RWV bioreactor, we harvested 3-D cellular aggregates for experimental analysis [25]. Prior to use in all assays, cell viability was measured as described above.

Ultrastructural Analyses

Samples were fixed and processed for scanning and transmission electron microscopy (TEM) as described previously [23]. Samples processed for TEM were imaged with a transmission electron microscope (model CM12; Philips), and images were acquired using a charge-coupled device camera and software (model 791; Gatan, Pleasanton, CA). Samples processed for scanning EM were imaged with a scanning electron microscope (Stereoscan 360 FE; Leica, Cambridge Co., Cambridge, U.K.) using EDS 2006 software (IXRF Systems Inc., Houston, TX).

Immunofluorescent Staining and Microscopy

Staining and microscopy were performed as previously described [25]. Briefly, cells were permeabilized with 0.1% Triton X-100 in Dulbecco phosphate-buffered saline, and blocked in 4% bovine serum albumin (BSA; Sigma-Aldrich) for 1 h at 37°C. The primary antibodies MUC1 (1:50 dilution; BD Pharmingen, San Jose, CA), epithelial-specific antigen (ESA; 1:50 dilution; Chemicon, Temecula, CA), and claudin-4 (1:200 dilution; Invitrogen) in 1% BSA were incubated with cells overnight at 4°C. Cells were washed and incubated for 1 h with the secondary antibody diluted 1:500 (Alexa Fluor 555; Invitrogen) and mounted in ProLong Gold antifade reagent with 4′,6-diamidino-2-phenylindole (DAPI; Molecular Probes; Invitrogen). Cells were imaged using an LSM 7 laser scanning confocal microscope (Zeiss) and analyzed using Zen 2009 Light Edition software.

MTT Assay for Determination of Cellular Viability after Nonoxynol-9 Treatment

ML or 3-D endocervical EC were seeded in 24-well plates and treated with 20, 50, 100, and 500 μg ml^{-1} nonoxynol-9 (N-9) or PBS (control). At 4 or 24 h post-treatment, an MTT (3-[4,5-dimethylthiazol-2-yl]-2,5-diphenyltetrazolium bromide) assay was performed as described previously [25]. Control treatments for each cell type were set at 100%.

Toll-Like Receptor Stimulation and Cytokine/Chemokine Quantification

The 3-D endocervical EC were seeded in 24-well plates and exposed to Toll-like receptor (TLR) agonists (InvivoGen) at 10 μg ml^{-1} CL097 (imidazoquinoline compound; TLR7/8 ligands), 5 μg ml^{-1} FLA-ST (purified flagellin from *Salmonella enterica* serovar Typhimurium; TLR5 ligand), 0.1 μg ml^{-1} FSL-1 (synthetic diacylated lipoprotein; TLR2/6 ligand), 10 μg ml^{-1} GARD (gardiquimod [$C_{17}H_{23}N_5O$], an imidazoquinoline compound; TLR7 ligand), 100 ng ml^{-1} LPS-SM (purified lipopolysaccharide from *Salmonella enterica* serovar Minnesota; TLR4 ligand), 5 μg ml^{-1} MPLA (monophosphoryl lipid A; TLR4 ligand), 5 μg ml^{-1} PAM_3CSK_4, (synthetic bacterial lipoprotein; TLR2/1 ligand), 5 μg ml^{-1} ODN2006 (type B cytosine-phosphate-guanine oligonucleotide; TLR9 ligand), and 25 μg ml^{-1} poly I:C (synthetic analog of double-stranded RNA; TLR3 ligand). Cellular supernatants (125 μl) were collected from each well 24 h poststimulation and stored at −20°C until analysis. Cytokine analysis was carried out by cytometric bead array using Pro Human custom cytokine assay (Bio-Plex) that contained the following targets: interleukin 6 (IL-6), IL-8, tumor necrosis factor-alpha (TNF-α), interferon-inducible protein 10 (IP-10 or CXCL10), and IL1 receptor antagonist (IL1-Ra) (Bio-Plex). Cytokine levels were quantified with a Bioplex-200 machine and analyzed by using version 5.0 manager software (Bio-Rad).

RT-PCR

RNA from ML and 3-D endocervical EC was extracted using the RNeasy kit (Qiagen, Valencia, CA) according to the manufacturer's instructions. RNA was quantified using a NanoDrop (Thermo Scientific, Rockford, IL). cDNA was generated from 2 μg of RNA by using iScript (BioRad, Hercules, CA) according to the manufacturer's instructions.

Relative gene expression of selected targets was measured by quantitative RT-PCR (qRT-PCR) analysis, performed with the model ABI 7500 system (Applied Biosystems, Foster City, CA). The 25-μl reaction mixture containing sample cDNA (20 ng), primer sets (300 nM), and FastStart Universal SYBR Green Master Mix with ROX (Roche, Indianapolis, IN) was added to each well in duplicate. Expression of human *GAPDH* was analyzed in each sample for normalization of total RNA. The sequence of the primers for each target gene is shown in Supplemental Table S1 (supplemental data are available online at www.biolreprod.org). The PCR cycle was as follows: 95°C for 10 min, followed by 40 cycles of 95°C for 15 sec and 55°C for 60 sec, followed by a melting curve analysis. Plasmids containing gene targets for standard controls were constructed according to Applied Biosystems protocol and as previously described [27]. Briefly, human endocervical cDNA was amplified using primer sets listed in Supplemental Table S1 and by ligating product into pGEM-T Easy vector system I (Promega, Madison, WI). To establish a standard curve, we serially diluted the plasmid constructed for each target by 10-fold and used 5 μl of each dilution in the PCR assay.

Statistics

All sample analyses were performed in duplicate unless otherwise stated. An unpaired two-tailed Student *t*-test was performed using Excel (Microsoft,

Redmond, WA) or Prism software (version 5.0d; GraphPad, San Diego, CA) analysis. P values of <0.05 were considered significant, and $P < 0.01$ was considered highly significant.

RESULTS

Tissue-Like Morphology and Ultrastructure of the 3-D Endocervical EC Model

To construct the 3-D endocervical EC model, we used RWV bioreactor technology and the previously characterized endocervical EC line A2EN [22, 24]. The A2EN cell line was chosen as a result of its primary-like phenotypes, including the expression of TLRs and innate immune mediators [24]. Endocervical EC were initially grown as ML and then introduced into the RWV bioreactor in combination with collagen-coated porous microcarrier beads [23, 25, 28]. The rotation of the bioreactor creates an environment of low fluid shear devoid of cellular sedimentation, and, as a result of this culture environment, cells attach to the beads and form tissue-like cellular aggregates by 28–32 days in culture. Electron microscopy examination of these RWV-generated endocervical EC aggregates revealed several hallmarks of cellular differentiation and polarity consistent with human endocervical tissue (Fig. 1) [2, 3, 17]. First, scanning EM images revealed a single layer of EC covering the beads with the characteristic ''cobblestone'' appearance at magnifications of 10× and 500× (Fig. 1A) [2, 3]. Magnification at 5000× also permitted visualization of surface and secreted cellular components. Subsequent evaluation of the 3-D endocervical EC aggregates by TEM (Fig. 1B) allowed for a more detailed analysis of the tissue-like ultrastructures that developed, including i) microvilli, ii) tight junctional complexes/desmosomes, and iii) secretory vesicles localizing at the cell surface. Taken together, these EM images demonstrated clear physical and structural similarities between the 3-D endocervical EC model and previously published EM images of human endocervical tissue [2, 3].

To more specifically evaluate and better define the ultrastructures observed in the EM images, we performed confocal immunofluorescence microscopy with both 3-D and ML endocervical EC (Fig. 1, C–E). To first distinguish apical-basal polarity or orientation of the endocervical EC, we labeled the cells with the basolateral marker ESA antibody (Fig. 1C) [29]. The ''honeycomb'' pattern staining observed in the aggregates suggested establishment of polarity and differentiation of the cells within the aggregate [2, 3]. In contrast, the staining pattern in monolayers was diffuse and did not localize to the outer cellular junctional complexes. The 3-D endocervical EC labeled with claudin-4, a major cell adhesion molecule of tight junctions [30], also displayed a honeycomb-like staining pattern, demonstrating the presence of tight junctional complexes between the EC of the aggregate that was not observed in the ML images (Fig. 1D). Taken together, these data indicate endocervical EC 3-D aggregates are polarized and exhibit in vivo-like localization of tight junctional complexes.

Secreted material observed on the surface of the aggregates in the SEM images (Fig. 1A) displayed physical characteristics of mucus, a critical player in establishing a protective barrier in the endocervix [12–14]. Mucins are a major component of mucus, and, using an antibody specific for a mucin known to be present in the FRT, MUC1, we analyzed ML and 3-D aggregates for MUC1 expression, using confocal microscopy (Fig. 1E) [12, 14]. MUC1 could only be detected by immunostaining in the 3-D EC aggregates. In addition, we quantified MUC1 surface expression on the 3-D EC aggregates by flow cytometry and determined that ~25.4% of the cells forming the aggregates expressed MUC1 on their surface (see Supplemental Fig. S1 and Supplemental Materials and Methods). These data suggested that MUC1 is expressed by the 3-D endocervical EC aggregates, and MUC1 is one potential component of the secreted material observed on the surface of the endocervical aggregates (Fig. 1A).

3-D Endocervical EC Possess Tight Junctional Complexes and In Vivo-Like Structural Barrier Properties

Endocervical EC form intercellular tight junctional complexes to maintain tissue integrity and establish an impermeable barrier [4]. Next, to test the EC ability to form tight junctional complexes of 3-D endocervical aggregates against a relevant destructive agent, we exposed them to the spermicidal detergent N-9 [31]. N-9 destroys tissue integrity and causes epithelial permeability in the FRT; therefore, we wanted to determine whether the 3-D model displayed levels of N-9 resistance similar to those previously documented for cervical explant tissue (Fig. 2) [31, 32]. ML and 3-D endocervical EC were exposed to various concentrations of N-9 for 4 or 24 h, and after each time point, cellular viability and metabolism were determined using the MTT assay. We found that 3-D endocervical cells maintained a significantly ($P < 0.05$ to $P < 0.01$) higher level of resistance to N-9 than the more susceptible ML cells and that this resistance was similar to epithelial permeability in cervical explants [32]. These data suggest that the junctional complexes of the 3-D endocervical aggregates function and contribute to the protective barrier necessary to maintain structure and function of the endocervix.

TLR Responsiveness to Microbial Products in 3-D Endocervical EC Aggregates

TLRs play a major role in maintaining the relatively microbe-free environment of the endocervix by sensing microbial products and eliciting an innate immune response. To determine whether the 3-D endocervical model possessed functioning and responsive TLRs, we exposed aggregates to a panel of TLR agonists (purified or synthetic microbial products) at previously published concentrations [23, 24, 33–35]. After 24 h of exposure, 3-D endocervical EC aggregates responded by proinflammatory cytokine secretion, specifically to TLR1/2, TLR3/5, and TLR2/6 agonists (Fig. 3, A–D). Endocervical EC aggregates also elicited an anti-inflammatory response with the production of IL1-Ra (Fig. 3E). Importantly, this pattern of TLR responsiveness is consistent with primary endocervical cells and endocervical tissue in which the previously published endocervical monolayer TLR responsiveness data can serve as a baseline for comparison [24, 36].

Mucin Expression Is Increased in Response to Microbial Products

Mucus is an essential and abundant component of mucosal surfaces as it serves to lubricate and protect the underlying mucosal surfaces [14, 18, 37]. EM images illustrating the globular and string-like material covering 3-D endocervical EC aggregates (Fig. 1A) and MUC1 expression as observed by confocal microscopy (Fig. 1E) suggested mucus-like material composed of MUC1 is being synthesized and secreted from the aggregates. To systematically profile the type and magnitude of mucins being expressed by the 3-D endocervical EC, we performed qRT-PCR analysis of our 3-D and ML endocervical EC (Fig. 4A). Similar to human endocervical tissue and cervical secretions, we observed *MUC1*, *MUC4*, *MUC5AC*, *MUC6*, and *MUC16* to be the most highly expressed mucins in

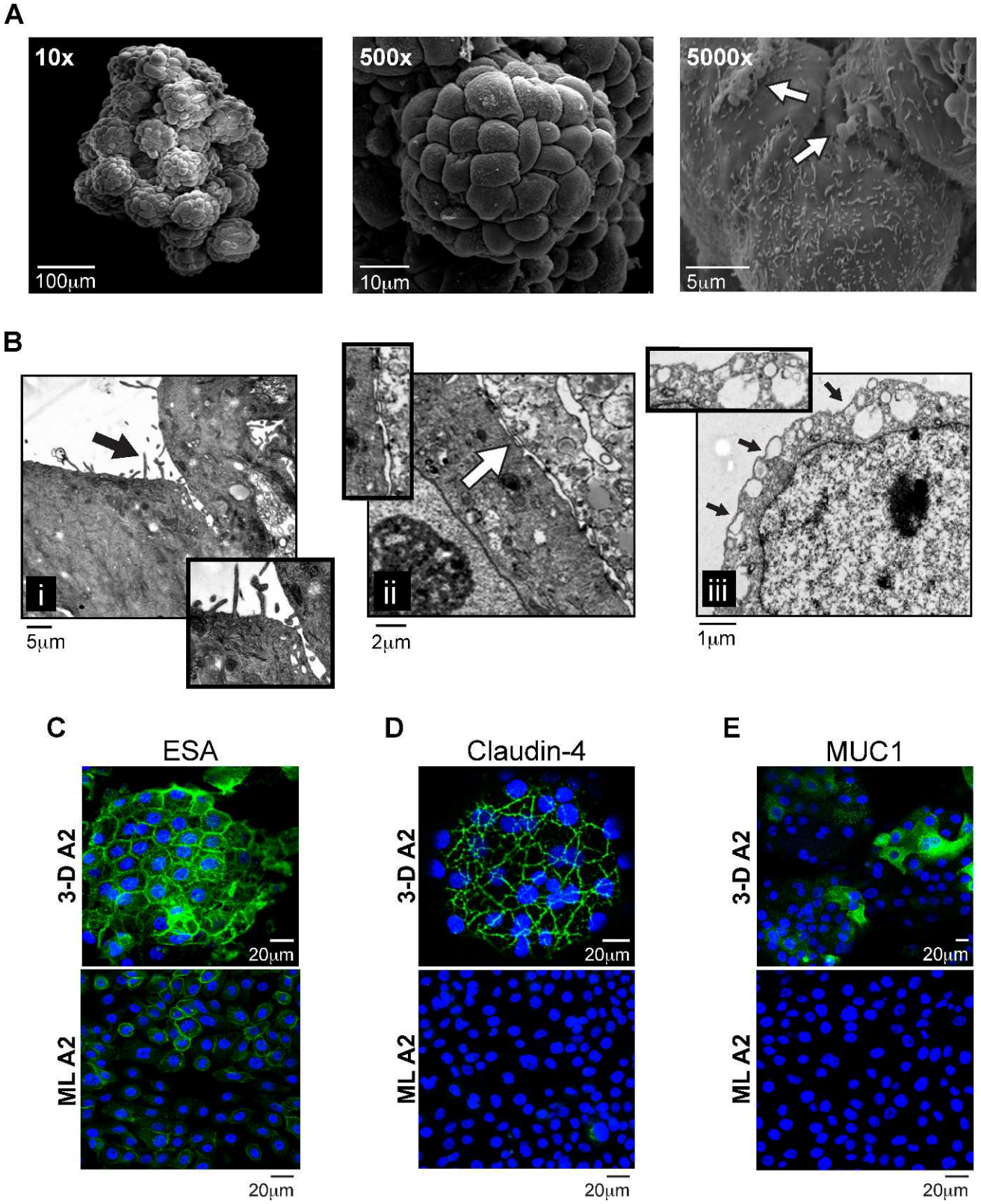

FIG. 1. Morphology and structural characteristics of 3-D endocervical EC. **A**) SEM images of a 3-D human endocervical EC aggregate at magnifications ×10, ×500, and ×5000. White arrow points to areas of mucus. **B**) TEM images of a 3-D endocervical EC aggregate. Insets highlight **i**) microvilli (black arrow), **ii**) tight junctional complexes (white arrow), and **iii**) secretory vesicles (black arrows). Confocal immunofluorescence microscopy images of 3-D endocervical EC (top panel) and confluent endocervical EC ML (bottom panel) were labeled with anti-ESA (**C**), anti-claudin-4 (**D**), and anti-MUC1 (**E**) antibodies and counterstained with DAPI to label nuclei.

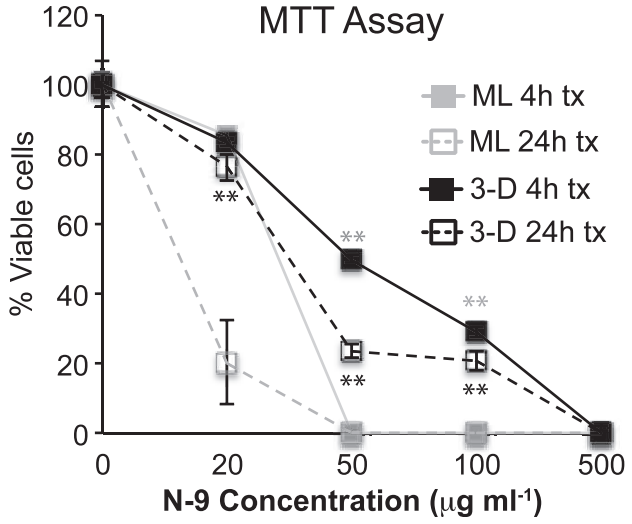

FIG. 2. Barrier capability of the tight junctional complexes in ML and 3-D endocervical EC. ML (gray lines) and 3-D (black) endocervical EC viability/active metabolism were determined by MTT assay following N-9 treatment for 4 h (solid lines) or 24 h (dashed lines). Points shown are representative mean ± SD values from triplicate samples from three independent experiments. Statistical comparisons were made between ML and 3-D EC at 4 and 24 h post-N-9 treatment for each concentration by using the Student *t*-test. $^{**}P < 0.01$ represents (black) 24-h treatment (tx) and (gray) 4-h.

the 3-D model, and these levels were significantly higher than those of ML cells [12, 19, 38, 39]. Expanding on the previously established mucin profile of the endocervix, we profiled additional mucins, including *MUC2*, *MUC3*, *and MUC17*, all of which were minimally expressed. In sum, these data demonstrate that this 3-D endocervical EC model exhibits a mucin profile similar to that of human endocervical tissue and secretions.

Next, we investigated whether 3-D endocervical EC could modulate mucin expression in response to microbial products. Aggregates were exposed to a panel of microbial products that activate specific TLRs for 24 h, and we observed a significant ($P < 0.05$) increase in *MUC1* expression in response to both viral (poly I:C) and bacterial (FLA, PAM_3CSK_4, and FSL-1) products (Fig. 4B). *MUC2*, *MUC3*, *MUC4*, *MUC5AC*, *MUC5B*, *MUC6*, *MUC16*, and *MUC17* were also systematically profiled for alterations in their expression levels upon microbial product stimulation. Interestingly, only *MUC1*, *MUC4*, and *MUC16* expression levels were significantly increased ($P < 0.05$) in response to poly I:C (viral product) treatment (Fig. 4, C and D). A TLR9 agonist (ODN2006) and TLR7/8 agonist (CL097) were used as a negative control as these TLR are expressed at low levels; however, we are only showing ODN2006 results for simplicity [24]. Exposure to ODN2006 did not alter mucin levels after stimulation, demonstrating TLR signaling specificity in altering mucin profiles. Taken together, these novel results demonstrate that microbial products differentially modulate the expression of membrane-associated mucins in endocervical EC.

3-D Endocervical EC Elicit a Distinct AMP Response to Specific Microbial Products

AMPs are a major innate defense mechanism at mucosal sites, but we know little about their induction and regulation in endocervical EC by microbial products. Using qRT-PCR, we therefore first profiled constitutive AMP expression in both ML and 3-D endocervical EC (Fig. 5A). For all AMPs profiled, 3-D endocervical EC expressed significantly ($P < 0.05$ to $P < 0.01$) higher levels of AMP than ML cells. Furthermore, the most highly expressed AMP in the 3-D endocervical aggregates (*SLPI*, *CCL20*, and *hBD1*) is consistent with expression patterns and levels (~0.1–1.0 μg ml^{-1}) observed in human endocervical mucus [40–43]. To investigate the effects of microbial products on AMP levels, we then exposed 3-D endocervical EC to the same panel of TLR agonists as described in Figure 4. Poly I:C exposure significantly ($P < 0.05$) increased only *hBD-1*, *hBD-2*, *SLPI*, and *CCL20* expression (Fig. 4, B–D, and Fig. 5, B–E), similar to the robust poly I:C-induced mucin expression. Exposure to bacterial products (FLA, PAM_3CSK_4, and FSL-1) also resulted in a significant increase of AMP, but the degree of modulation was dependent upon the specific microbial product. Taken together, our data suggest unique innate immune signatures emerge in the endocervix depending on the specific microbial product. These innate mediators not only respond to protect the host against pathogens but also fluctuate to maintain and regain homeostasis of the endocervix.

DISCUSSION

Here we describe the development of a 3-D human organotypic endocervical EC model that possesses many functional and structural characteristics analogous to those of the human endocervix. Using an RWV bioreactor culture system, we generated 3-D endocervical EC aggregates that displayed the hallmarks of differentiation (tight junctional complexes, secretory vessels, microvilli) as well as mucosal surface-specific innate immune receptors and mucins (Figs. 1–3) [2–4, 7, 24, 36]. Upon further characterization of the secretory material produced by the aggregates, we detected a mucin expression profile similar to that identified in human endocervical tissues and secretions (Fig. 4) [12, 13, 19, 38, 39]. The expression profile of AMPs produced by the 3-D endocervical aggregates was also consistent with AMP expression detected in cervical secretions (Fig. 5) [6, 40–42]. Hence, this model provides a unique resource to simultaneously study human mucin, AMP, and pathogen interactions. We also report, for the first time, that microbial products significantly up-regulated expression of the transmembrane mucins *MUC1*, *MUC4*, and *MUC16* in the endocervix. AMPs that have been identified in human cervical secretions in vivo were also up-regulated in the 3-D endocervical EC aggregates upon bacterial and viral product stimulation, including *CCL20*, *SLPI*, *hBD-1*, and *hBD-2* [6, 40–42, 44]. Mucin and AMP expression levels were each distinctively modulated by the panel of microbial products tested, suggesting endocervical EC selectively respond to specific microbes.

Our study highlights the dynamic interactions that occur among microbial products and mucins produced by EC. Understanding of microbe-mucin interactions is important, as these interactions occur at every mucosal site in the body and influence diverse cellular processes, such as innate immunity, microbiome microbial inhabitants, and cellular homeostasis [1, 18, 45, 46]. We provide a novel insight into how endocervical EC specifically respond to microbial products by altering their mucin levels. The viral double-stranded RNA mimic poly I:C caused substantial increases in transmembrane mucins *MUC1*, *MUC4*, and *MUC16* expression levels in 3-D endocervical EC aggregates. *MUC1*, *MUC4*, and *MUC16* specifically are known to play a critical role in lubricating and hydrating ocular surfaces, as well as in preventing pathogen penetrance into the eye [47, 48]. Despite the fact that we profiled both the

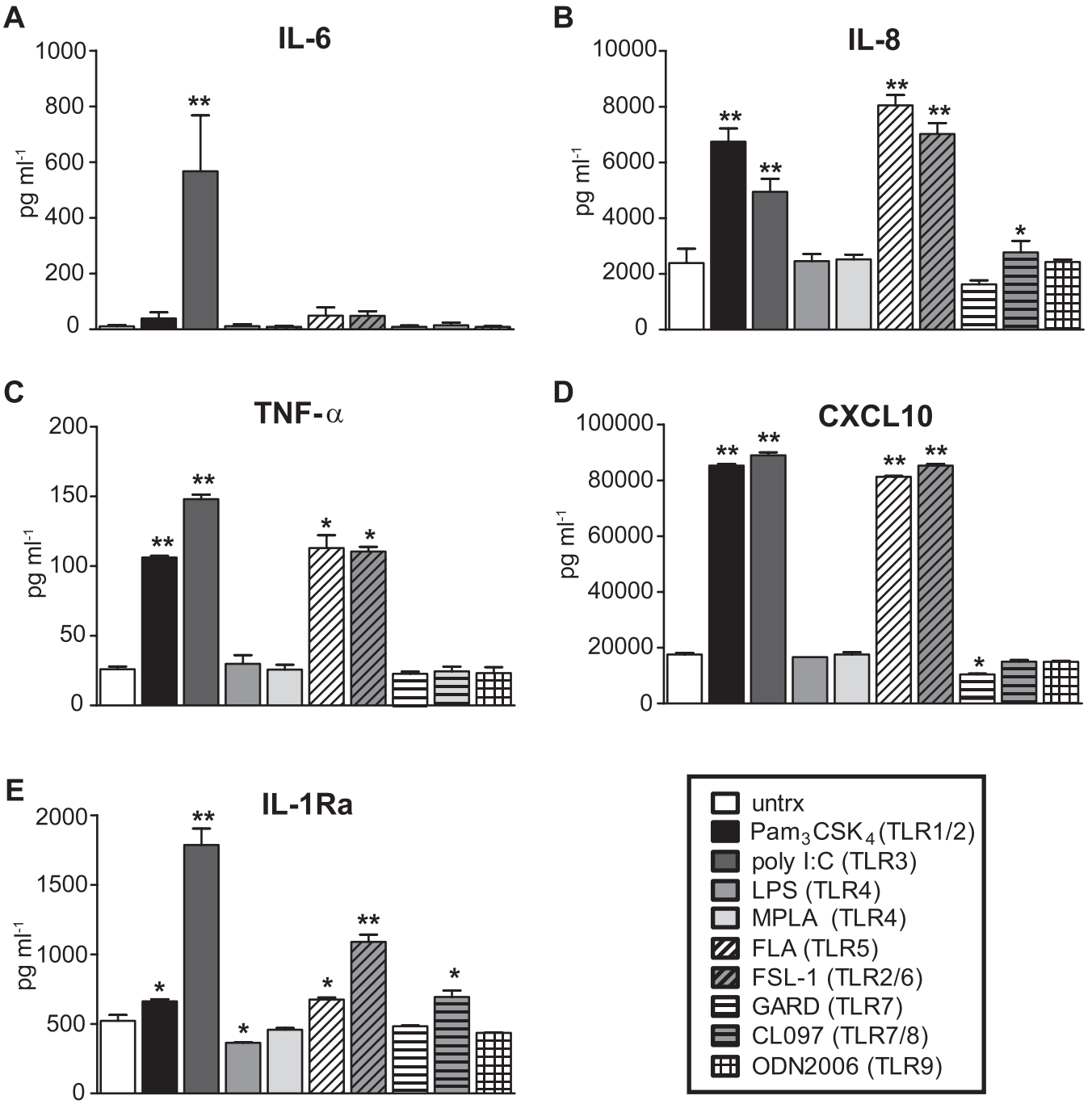

FIG. 3. Cytokine production from 3-D endocervical EC following microbial product exposure. Cytokine levels produced by 3-D endocervical EC 24 h poststimulation with a customized panel of TLR agonists were compared to untreated (untrx) EC. IL-6 (**A**), IL-8 (**B**), TNF-α (**C**), CXCL10 (**D**), and IL-1Ra (**E**). Cytokine and chemokine values shown are representative mean ± SD levels from duplicate samples from three independent experiments. Statistical comparisons were made between TLR agonist treated EC versus untreated EC for each cytokine measured by using the Student *t*-test. $*P < 0.05$; $**P < 0.01$.

membrane-associated and secreted mucins, only cell-associated mucins (*MUC1*, *MUC4*, and *MUC16*) were up-regulated. Interestingly, we did not identify any alterations in the expression of gel-forming mucins upon microbial product exposure, and this could be the result of regulation or modification at the protein level. For example, TNF-α has been shown to induce release of *MUC1*, *MUC4*, and *MUC16* from the membrane, resulting in the soluble forms of the proteins to be present in tears [47]. In the 3-D endocervical model, poly I:C was shown to significantly increase TNF-α production (Fig. 3). Taken together with our knowledge of ocular mucosal surfaces, TNF-α production following poly I:C exposure could potentially cause a release of *MUC1*, *MUC4*, and *MUC16* from the 3-D endocervical EC aggregate membrane, creating a disadhesive barrier [45, 47]. The observed increased synthesis of these mucins may be a result of the cell replenishing these membrane-associated mucins released upon cytokine exposure.

The functions of each mucin are dependent upon their location in the body, and the protective barrier function of mucin observed on ocular surfaces might not serve the same protective role in the endocervix. Here, we focus our discussion

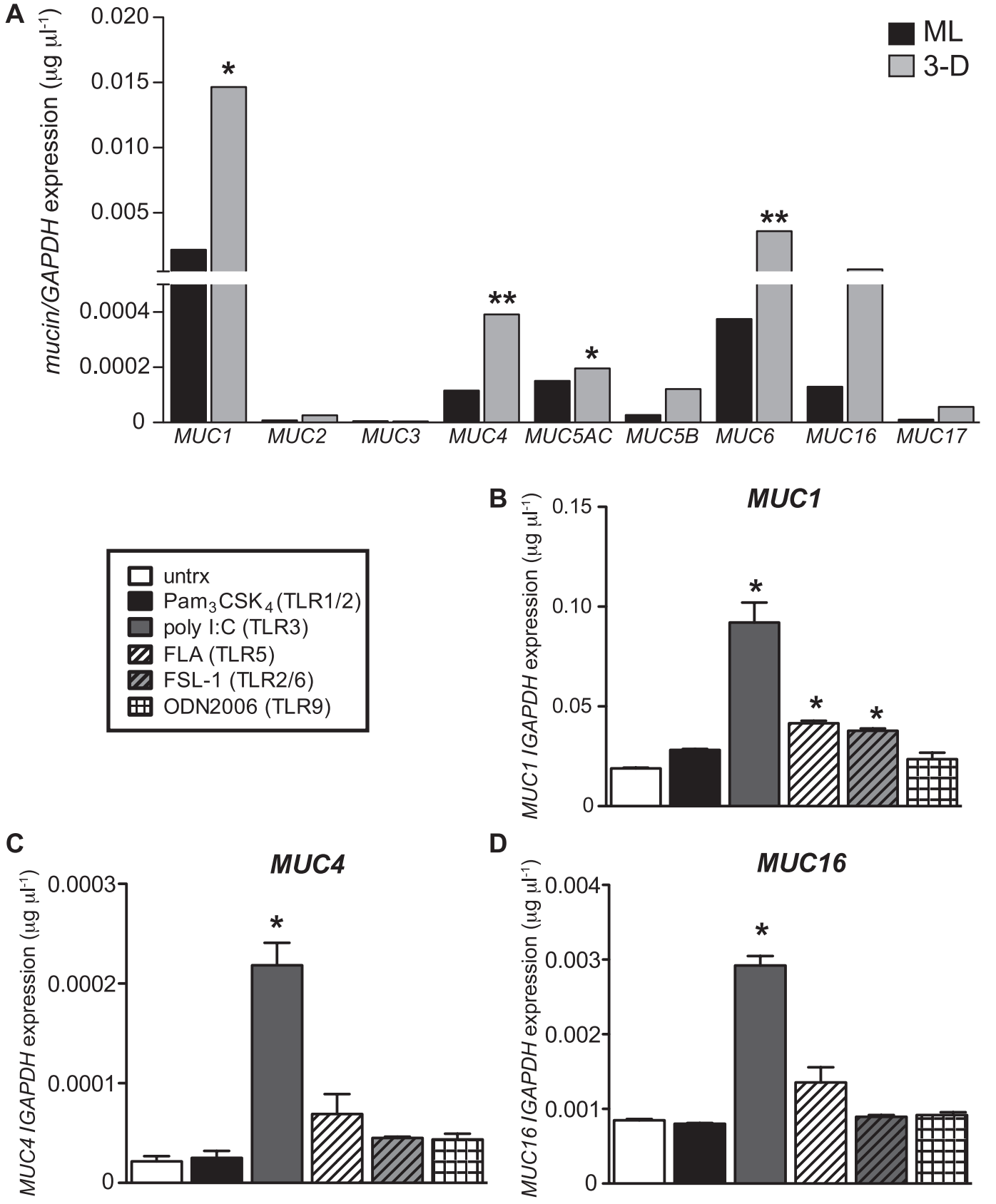

FIG. 4. Mucin expression in 3-D endocervical EC after microbial product stimulation. **A**) ML and 3-D endocervical EC were profiled for mucins by qRT-PCR analysis. Statistical comparisons were made between ML and 3-D endocervical EC for each gene, using the Student *t*-test. 3-D endocervical EC *MUC1* (**B**), *MUC4* (**C**), and *MUC16* (**D**) expression 24 h postexposure with TLR agonists. All gene expression was normalized to that of *GAPDH*. Expression levels shown are representative mean ± SD values from duplicate samples from at least three independent experiments. Statistical comparisons were made between untreated (untrx) and TLR agonist-treated EC by using the Student *t*-test. $^{*}P < 0.05$; $^{**}P < 0.01$.

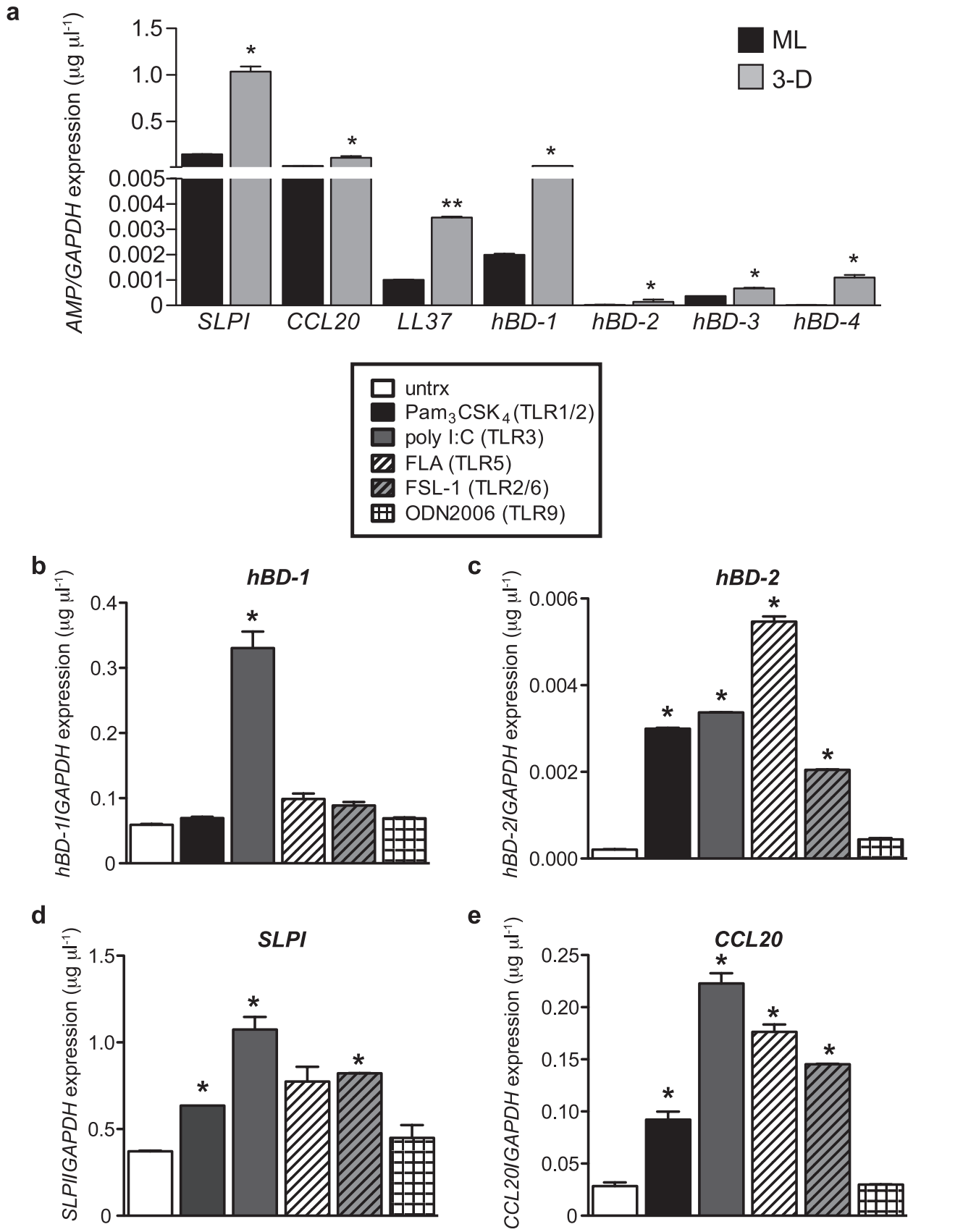

FIG. 5. Elevated expression of AMPs in 3-D endocervical EC after microbial product stimulation. **A**) ML and 3-D endocervical EC aggregates were profiled for mucins by qRT-PCR analysis. Statistical comparisons were made between ML and 3-D endocervical EC for each gene using the Student *t*-test. 3-D endocervical EC *hBD-1* (**B**), *hBD-2* (**C**), *SLPI* (**D**), and *CCL20* (**E**) expression at 24 h postexposure with TLR agonists. All gene expression was normalized to that of *GAPDH*. Representative expression levels shown are the mean ± SD values from duplicate samples from at least three independent experiments. Statistical comparisons were made between untreated (untrx) and TLR agonist-treated EC by using the Student *t*-test. $*P < 0.05$; $**P < 0.01$.

on the protective function of mucin in response to pathogen exposure in the endocervix, but it is known that mucin also plays a role in reproduction [2, 49]. This site-specific difference in mucin function is also highlighted in the GI and respiratory tracts, in which numerous studies suggest that mucus covering these sites functions more as a pathogen receptor than a protective barrier [18, 37, 46]. Similar to GI and respiratory tract pathogens that ''hijack'' mucosa to establish infections, numerous sexually transmitted infection pathogens, including *Neisseria gonorrhoeae*, *Chlamydia trachomatis*, and *Trichomonas vaginalis*, also selectively adhere to mucins and produce proteases that degrade mucins and host defense components within the mucus [14, 18, 46, 50]. In addition, cervical mucus has been shown to significantly slow the diffusion rate of herpes simplex virus (HSV) compared to a PBS control liquid, although mucus had no effect on human papilloma virus (HPV) diffusion rate [51, 52]. Development of sexually transmitted infection models in this mucus-producing 3-D endocervical EC system will help to further elucidate the mucus-pathogen interactions specific to this site.

Endocervical mucus may also contribute to an effective endocervical innate immune response by housing a diverse array of nonspecific AMPs [1, 14, 18]. Upon systematic profiling of our 3-D endocervical EC aggregates, we identified relatively high constitutive levels of AMP, similar to those found in endocervical tissues and secretions (Fig. 4) [40–43]. However, only *SLPI*, *CCL20*, *hBD-1*, and *hBD-2* levels were altered upon exposure to microbial products. Interestingly, *CCL20* and *hBD-2* but not *SPLI* levels were found to be increased in cervicovaginal secretions of women with sexually transmitted infections [42, 53–55]. *SLPI* concentrations were correlated with reduced rates of perinatal HIV-1 transmission, suggesting SLPI is important in creating a pathogen-resistant environment [42, 54]. In preliminary HSV-2 infection studies with 3-D endocervical EC aggregates, *SLPI* expression was decreased following infection (Radtke and Herbst-Kralovetz, unpublished data), therefore demonstrating *SLPI* modulation may be dependent upon the stimuli (live pathogen versus purified viral product).

The urogenital tract, which includes the endocervix, is among the tissues of the body shown to express the highest levels of *hBD-1* [56]. *HBD-1* expression is considered to be constitutive at these sites, unlike *hBD-2* expression, which is predominantly induced at sites of inflammation (Fig. 5) [56]. Similar to recent studies using polarized endocervical EC and uterine EC, we provide data that shows *hBD-1* expression is induced upon poly I:C exposure [22, 33].

TLR3 activation by poly I:C has been shown to result in a cascade of defense signaling pathways that induce the activation of NF-κβ, interferon production, cytokine/chemokine secretion, and, most recently, AMP expression alterations in the FRT [22, 57]. We have extended those studies by analyzing the effects of bacterial lipoproteins (Pam_3CSK_4, FSL-1) and flagellin (FLA) on these expression levels. We showed that modulation of the AMP expression profile was dependent upon the viral or bacterial product used and that no standard immune signature is demonstrated (Figs. 4 and 5). We further expanded the innate defense gene profiling of the 3-D endocervical EC aggregates by monitoring changes in mucin expression after microbial product stimulation. Interestingly, poly I:C stimulation resulted in the most profound and consistent increase in membrane-associated mucin expression, whereas bacterial products did not induce such dramatic alterations (Fig. 4). This viral product-induced increase in mucin could potentially serve as a protection mechanism for the host [51, 52]. In contrast, the modest changes in mucin expression following exposure to bacterial products could serve to protect the EC by providing an environment that does not promote bacterial adhesion and infection as previously discussed [14, 18]. These findings demonstrate a unique innate defense signature produced by the 3-D endocervical aggregates in response to specific microbial products. Further studies need to be conducted using live viral and bacterial pathogens to confirm these signatures.

The structure, function, and immune responsiveness of the complex biosystem of cells that form the FRT are greatly influenced by the mucosal environment. Our data show that EC grown under a physiologically low fluid shear environment in an RWV bioreactor results in mucin, AMP expression, and responses to microbial products that are similar to in vivo human tissue. However, the 3-D endocervical model is not limited to the study of innate immune mechanisms, and our model can be modified to recapitulate different FRT microenvironments (which vary in pH, hormone effect, cellular complexity, commensal microflora, and other characteristics). Together with our previously published 3-D vaginal EC model [23], we have the capability to study site-specific differences in FRT biology. Studies with our 3-D FRT models can now be expanded but not limited to such areas as hormone regulation, novel therapeutics, genital microbiome, fertility/reproduction, cancer biology, and other disciplines that would benefit from an organotypic model system that accurately predicts human FRT tissue responses.

ACKNOWLEDGMENT

We would like to thank Erin Jackson for cell culture support and Kyle Abraham and Dave Lowry for assistance in the preparation and generation of TEM images. We acknowledge St. Joseph's Hospital and Medical Center and the UA Department of Basic Medical Sciences for use of core equipment.

REFERENCES

1. Hickey DK, Patel MV, Fahey JV, Wira CR. Innate and adaptive immunity at mucosal surfaces of the female reproductive tract: stratification and integration of immune protection against the transmission of sexually transmitted infections. J Reprod Immunol 2011; 88:185–194.
2. Hafez ESE. Structural and ultrastructural parameters of the uterine cervix. Obstet Gynecol Surv 1982; 37:507–516.
3. Ludwig H, Metzger, H. The Human Female Reproductive Tract: A Scanning Electron Microscopy Atlas. New York: Springer-Verlag; 1979.
4. Blaskewicz CD, Pudney J, Anderson DJ. Structure and function of intercellular junctions in human cervical and vaginal mucosal epithelia. Biol Reprod 2011; 85:97–104.
5. Kaushic C, Nazli A, Ferreira VH, Kafka JK. Primary human epithelial cell culture system for studying interactions between female upper genital tract and sexually transmitted viruses, HSV-2 and HIV-1. Methods 2011; 55: 114–121.
6. Horne AW, Stock SJ, King AE. Innate immunity and disorders of the female reproductive tract. Reproduction 2008; 135:739–749.
7. Nasu K, Narahara H. Pattern recognition via the toll-like receptor system in the human female genital tract. Mediators Inflamm 2010; 2010:976024.
8. Wira CR, Fahey JV, Sentman CL, Pioli PA, Shen L. Innate and adaptive immunity in female genital tract: cellular responses and interactions. Immunol Rev 2005; 206:306–335.
9. Heinonen PK, Teisala K, Punnonen R, Miettinen A, Lehtinen M, Paavonen J. Anatomic sites of upper genital tract infection. Obstet Gynecol 1985; 66:384–390.
10. Espinoza J, Erez O, Romero R. Preconceptional antibiotic treatment to prevent preterm birth in women with a previous preterm delivery. Am J Obstet Gynecol 2006; 194:630–637.
11. Quayle AJ. The innate and early immune response to pathogen challenge in the female genital tract and the pivotal role of epithelial cells. J Reprod Immunol 2002; 57:61–79.
12. Gipson IK. Mucins of the human endocervix. Front Biosci 2001; 6: D1245–D1255.
13. Carson DD, DeSouza MM, Kardon R, Zhou X, Lagow E, Julian J. Mucin

expression and function in the female reproductive tract. Hum Reprod Update 1998; 4:459–464.
14. DeSouza MM, Lagow E, Carson DD. Mucin functions and expression in mammalian reproductive tract tissues. Biochem Biophys Res Commun 1998; 247:1–6.
15. Yurewicz EC, Moghissi KS. Purification of human midcycle cervical mucin and characterization of its oligosaccharides with respect to size, composition, and microheterogeneity. J Biol Chem 1981; 256: 11895–11904.
16. Carlstedt I, Sheehan JK, Corfield AP, Gallagher JT. Mucous glycoproteins: a gel of a problem. Essays Biochem 1985; 20:40–76.
17. Wergin WP. Cyclic changes in the surface structure of the cervix from the ewe as revealed by scanning electron microscopy. Tissue Cell 1979; 11: 359–370.
18. McGuckin MA, Linden SK, Sutton P, Florin TH. Mucin dynamics and enteric pathogens. Nat Rev Microbiol 2011; 9:265–278.
19. Gipson IK, Ho SB, Spurr-Michaud SJ, Tisdale AS, Zhan Q, Torlakovic E, Pudney J, Anderson DJ, Toribara NW, Hill JA III. Mucin genes expressed by human female reproductive tract epithelia. Biol Reprod 1997; 56: 999–1011.
20. Ganz T. Defensins: antimicrobial peptides of innate immunity. Nat Rev Immunol 2003; 3:710–720.
21. Wira CR, Ghosh M, Smith JM, Shen L, Connor RI, Sundstrom P, Frechette GM, Hill ET, Fahey JV. Epithelial cell secretions from the human female reproductive tract inhibit sexually transmitted pathogens and *Candida albicans* but not *Lactobacillus*. Mucosal Immunol 2011; 4: 335–342.
22. Buckner LR, Schust DJ, Ding J, Nagamatsu T, Beatty W, Chang TL, Greene SJ, Lewis ME, Ruiz B, Holman SL, Spagnuolo RA, Pyles RB, et al. Innate immune mediator profiles and their regulation in a novel polarized immortalized epithelial cell model derived from human endocervix. J Reprod Immunol 2011; 92:8–20.
23. Hjelm BE, Berta AN, Nickerson CA, Arntzen CJ, Herbst-Kralovetz MM. Development and characterization of a three-dimensional organotypic human vaginal epithelial cell model. Biol Reprod 2010; 82:617–627.
24. Herbst-Kralovetz MM, Quayle AJ, Ficarra M, Greene S, Rose WA II, Chesson R, Spagnuolo RA, Pyles RB. Quantification and comparison of toll-like receptor expression and responsiveness in primary and immortalized human female lower genital tract epithelia. Am J Reprod Immunol 2008; 59:212–224.
25. Radtke AL, Herbst-Kralovetz, MM. Culturing and applications of rotating wall vessel bioreactor derived 3d epithelial cell models. J Vis Exp 2012; 62:e3868.
26. Barrila J, Radtke AL, Crabbe A, Sarker SF, Herbst-Kralovetz MM, Ott CM, Nickerson CA. Organotypic 3D cell culture models: using the rotating wall vessel to study host-pathogen interactions. Nat Rev Microbiol 2010; 8:791–801.
27. Sivaganesan M, Seifring S, Varma M, Haugland RA, Shanks OCA. Bayesian method for calculating real-time quantitative PCR calibration curves using absolute plasmid DNA standards. BMC Bioinformatics 2008; 9:120.
28. Bernacki SH, Nelson AL, Abdullah L, Sheehan JK, Harris A, Davis CW, Randell SH. Mucin gene expression during differentiation of human airway epithelia in vitro. Muc4 and muc5b are strongly induced. Am J Respir Cell Mol Biol 1999; 20:595–604.
29. Schmeichel KL, Bissell MJ. Modeling tissue-specific signaling and organ function in three dimensions. J Cell Sci 2003; 116:2377–2388.
30. Tsukita S, Furuse M. Claudin-based barrier in simple and stratified cellular sheets. Curr Opin Cell Biol 2002; 14:531–536.
31. Hillier SL, Moench T, Shattock R, Black R, Reichelderfer P, Veronese F. In vitro and in vivo: the story of nonoxynol 9. J Acquir Immune Defic Syndr 2005; 39:1–8.
32. Beer BE, Doncel GF, Krebs FC, Shattock RJ, Fletcher PS, Buckheit RW Jr, Watson K, Dezzutti CS, Cummins JE, Bromley E, Richardson-Harman N, Pallansch LA, et al. In vitro preclinical testing of nonoxynol-9 as potential anti-human immunodeficiency virus microbicide: a retrospective analysis of results from five laboratories. Antimicrob Agents Chemother 2006; 50:713–723.
33. Schaefer TM, Fahey JV, Wright JA, Wira CR. Innate immunity in the human female reproductive tract: antiviral response of uterine epithelial cells to the TLR3 agonist poly(I:C). J Immunol 2005; 174:992–1002.
34. Trifonova RT, Doncel GF, Fichorova RN. Polyanionic microbicides modify Toll-like receptor-mediated cervicovaginal immune responses. Antimicrob Agents Chemother 2009; 53:1490–1500.
35. McGowin CL, Ma L, Martin DH, Pyles RB. *Mycoplasma genitalium*-encoded MG309 activates NF-kappaB via Toll-like receptors 2 and 6 to elicit proinflammatory cytokine secretion from human genital epithelial cells. Infect Immun 2009; 77:1175–1181.
36. Fazeli A, Bruce C, Anumba DO. Characterization of Toll-like receptors in the female reproductive tract in humans. Hum Reprod 2005; 20: 1372–1378.
37. Hansson GC. Role of mucus layers in gut infection and inflammation. Curr Opin Microbiol 2012; 15:57–62.
38. Gipson IK, Spurr-Michaud S, Moccia R, Zhan Q, Toribara N, Ho SB, Gargiulo AR, Hill JA III. MUC4 and MUC5B transcripts are the prevalent mucin messenger ribonucleic acids of the human endocervix. Biol Reprod 1999; 60:58–64.
39. Andersch-Bjorkman Y, Thomsson KA, Holmen Larsson JM, Ekerhovd E, Hansson GC. Large scale identification of proteins, mucins, and their O-glycosylation in the endocervical mucus during the menstrual cycle. Mol Cell Proteomics 2007; 6:708–716.
40. Moriyama A, Shimoya K, Ogata I, Kimura T, Nakamura T, Wada H, Ohashi K, Azuma C, Saji F, Murata Y. Secretory leukocyte protease inhibitor (SLPI) concentrations in cervical mucus of women with normal menstrual cycle. Mol Hum Reprod 1999; 5:656–661.
41. Hein M, Valore EV, Helmig RB, Uldbjerg N, Ganz T. Antimicrobial factors in the cervical mucus plug. Am J Obstet Gynecol 2002; 187:137–144.
42. Ghosh M, Fahey JV, Shen Z, Lahey T, Cu-Uvin S, Wu Z, Mayer K, Wright PF, Kappes JC, Ochsenbauer C, Wira CR. Anti-HIV activity in cervical-vaginal secretions from HIV-positive and -negative women correlate with innate antimicrobial levels and IgG antibodies. PLoS One 2010; 5:e11366.
43. Zegels G, Van Raemdonck GA, Coen EP, Tjalma WA, Van Ostade XW. Comprehensive proteomic analysis of human cervical-vaginal fluid using colposcopy samples. Proteome Sci 2009; 7:17.
44. Li Z, Palaniyandi S, Zeng R, Tuo W, Roopenian DC, Zhu X. Transfer of IgG in the female genital tract by MHC class I-related neonatal Fc receptor (FcRn) confers protective immunity to vaginal infection. Proc Natl Acad Sci U S A 2011; 108:4388–4393.
45. Govindarajan B, Gipson IK. Membrane-tethered mucins have multiple functions on the ocular surface. Exp Eye Res 2010; 90:655–663.
46. Lillehoj EP, Hyun SW, Kim BT, Zhang XG, Lee DI, Rowland S, Kim KC. Muc1 mucins on the cell surface are adhesion sites for *Pseudomonas aeruginosa*. Am J Physiol Lung Cell Mol Physiol 2001; 280:L181–187.
47. Blalock TD, Spurr-Michaud SJ, Tisdale AS, Gipson IK. Release of membrane-associated mucins from ocular surface epithelia. Invest Ophthalmol Vis Sci 2008; 49:1864–1871.
48. Gipson IK, Spurr-Michaud S, Argueso P, Tisdale A, Ng TF, Russo CL. Mucin gene expression in immortalized human corneal-limbal and conjunctival epithelial cell lines. Invest Ophthalmol Vis Sci 2003; 44: 2496–2506.
49. Hey NA, Meseguer M, Simon C, Smorodinsky NI, Wreschner DH, Ortiz ME, Aplin JD. Transmembrane and truncated (SEC) isoforms of MUC1 in the human endometrium and Fallopian tube. Reprod Biol Endocrinol 2003; 1:2.
50. Wiggins R, Hicks SJ, Soothill PW, Millar MR, Corfield AP. Mucinases and sialidases: their role in the pathogenesis of sexually transmitted infections in the female genital tract. Sex Transm Infect 2001; 77:402–408.
51. Lai SK, Wang YY, Hida K, Cone R, Hanes J. Nanoparticles reveal that human cervicovaginal mucus is riddled with pores larger than viruses. Proc Natl Acad Sci U S A 2010; 107:598–603.
52. Olmsted SS, Padgett JL, Yudin AI, Whaley KJ, Moench TR, Cone RA. Diffusion of macromolecules and virus-like particles in human cervical mucus. Biophys J 2001; 81:1930–1937.
53. Draper DL, Landers DV, Krohn MA, Hillier SL, Wiesenfeld HC, Heine RP. Levels of vaginal secretory leukocyte protease inhibitor are decreased in women with lower reproductive tract infections. Am J Obstet Gynecol 2000; 183:1243–1248.
54. Pillay K, Coutsoudis A, Agadzi-Naqvi AK, Kuhn L, Coovadia HM, Janoff EN. Secretory leukocyte protease inhibitor in vaginal fluids and perinatal human immunodeficiency virus type 1 transmission. J Infect Dis 2001; 183:653–656.
55. Ghosh M, Shen Z, Schaefer TM, Fahey JV, Gupta P, Wira CR. CCL20/MIP3alpha is a novel anti-HIV-1 molecule of the human female reproductive tract. Am J Reprod Immunol 2009; 62:60–71.
56. Cole AM. Innate host defense of human vaginal and cervical mucosae. Curr Top Microbiol Immunol 2006; 306:199–230.
57. Alexopoulou L, Holt AC, Medzhitov R, Flavell RA. Recognition of double-stranded RNA and activation of NF-kappaB by Toll-like receptor 3. Nature 2001; 413:732–738.